Adaptive Recovery of a Doppler Shifted Mobile Communications Signal Using the RLS Algorithm*

Paul Wei†, James R. Zeidler†‡, and Walter H. Ku†
†Department of Electrical and Computer Engineering,
University of California at San Diego, La Jolla, CA 92093-0407.
‡ Naval Command, Control and Ocean Surveillance Center
RDT& E Division, Code 804, San Diego, CA 92152-5000

Abstract *This paper studies the ability of the exponentially weighted RLS algorithm to track a doppler shifted BPSK communications signal. This is modeled as a chirped AR1 process in gaussian white noise. Expressions for the optimum Wiener filter, noise misadjustment, and lag misadjustment are shown. It is shown that as in the chirped sinusoid case the error can be written in terms of the forgetting rate $\beta = 1-\lambda$ of the RLS algorithm; the noise misadjustment is of the order β and lag misadjustment of order $1/\beta^2$. However, as the bandwidth of the signal increases the relative lag misadjustment is shown to decrease.*

1 Introduction

Adaptive filters have been extensively studied in a variety of stationary environments. Some applications include adaptive equalization, channel estimation, adaptive line enhancement, and interference suppression, all of which rely on the analysis of the underlying adaptive estimation algorithms in the stationary environment [1]. However in nonstationary *input* situations few cases have been analyzed. One method used by previous authors to analyze algorithm performance in the nonstationary environment (LMS [2], RLS [3]) was to model the optimum weights as a first order Markov process. This approach, however, lacks the physical insights into the causes and influences of the nonstationarity parameters on algorithm performance. Inroads into the analysis of the effects of *input* nonstationarity on algorithm performance were pioneered in [4,5], using a deterministic chirp input. This allows the design of the filter to be directly determined by the signal parameters.

*This work was supported by the NSF I/UC Research Center on Ultra High Speed Integrated Circuits and Systems (ICAS) at the University of California, San Diego, The Office of Naval Research and the National Science Foundation under grant #ECD89-16669.

The case of the chirp is of particular importance in the mobile communication environment where a linear shift in frequency can be used as a first order model for the doppler effect. This work extends the previous studies for the chirped tone to the more general chirped signal. The importance of having a nonzero bandwidth signal is that it more closely resembles a communications signal, since a zero bandwidth signal is *deterministic* and contains no information. In this paper the correspondence between the stationary signal and chirped signal results of RLS adaptive filter are shown to be related by a chirp matrix and a signal direction vector. As previously shown in the deterministic chirp analysis the adaptive filter tracks the input signal, with a lag component which increases as the adaptation parameter β is decreased. In addition this analysis will show that the lag misadjustment decreases as a function of signal bandwidth. At the output, the power consist of a component which depends only on the parameters of the *stationary* signal and a lag component which is a function of the chirp rate ψ. The properties of the lag component are derived as a function of the MA signal parameters. The analytical results obtained for the AR1 signal model are shown via simulation to describe the tracking performance of the RLS filter for a BPSK input signal.

2 Signal Model

Consider a moving average (MA) model of a stationary baseband communications signal

$$s_k = \sqrt{P_s} \sum_{l=-\infty}^{k} a_{k-l}\, u_l \qquad (1)$$

where $\{u_l\}$ is a white noise process with variance $\sigma_u^2 = 1$. The covariance matrix of this stationary signal is given by

$$\mathbf{\Phi}^s = P_s \mathbf{R} \qquad (2)$$

where $\mathbf{R} = E[\bar{s}^* \bar{s}^T]/P_s$ is the covariance matrix normalized by the signal power (P_s). The signal vector is given by $\bar{s}_k = [s_{k-1}, \ldots, s_{k-M}]^T$. The elements of $\mathbf{R}$ are given by $(\mathbf{R})_{i,j} = r_{i-j}$ where

$$r_m = \sum_{l=0}^{\infty} a_l a_{l+m}. \tag{3}$$

is the normalized autocorrelation function of the stationary MA signal.

To model the signal in a nonstationary mobile communication environment the signal spectrum may be frequency offset and shifted with time, by multiplying each term by a time dependent frequency shift and chirp term to give

$$s_k = \sqrt{P_s} \sum_{l=-\infty}^{k} a_{k-l} \Omega^{k-l} \Psi^{(k^2-l^2)/2} u_l \tag{4}$$

where $\Omega = e^{j\omega}$ shifts the center frequency of the spectrum and $\Psi = e^{j\psi}$ linearly shifts the center frequency with time. This simplifies to the deterministic chirp [4] when the stationary signal is a constant DC signal (ie: $a_k = 1$, and $u_l = \delta_l$), and (4) reduces to

$$s_k = \sqrt{P_s} \Omega^k \Psi^{k^2/2}. \tag{5}$$

The signal correlation $\mathbf{\Phi}_k^s$ is

$$E[s_k^* s_{k-m}] = r_m \left(\Omega^{-m} \Psi^{-mk}\right) \Psi^{m^2/2}. \tag{6}$$

By defining a new operator $\otimes$ to indicate *element by element multiplication*, the input signal correlation can be written in matrix notation as

$$\begin{aligned} \mathbf{\Phi}_k^s &= E[\bar{s}_k^* \bar{s}_k^T] \\ &= P_s \mathbf{R} \otimes (\mathbf{V}^k \bar{\mathrm{D}} \bar{\mathrm{D}}^H \mathbf{V}^{*k}), \end{aligned} \tag{7}$$

where $\bar{s}_k = [s_{k-1}, \ldots s_{k-M}]^T$ is the input signal vector and $\mathbf{R}$ is the correlation matrix of the stationary MA process with elements given by $(\mathbf{R})_{i,j} = r_{i-j}$. The matrix $\mathbf{V}$ is the *chirp matrix* and $\bar{\mathrm{D}}$ is the *signal direction* given by

$$\begin{aligned} \mathbf{V} &= diag(\Psi, \Psi^2, \ldots, \Psi^m) \\ \bar{\mathrm{D}} &= [\Omega \Psi^{-1/2}, \Omega^2 \Psi^{-2^2/2}, \ldots, \Omega^M \Psi^{-M^2/2}]^T. \end{aligned} \tag{8}$$

At the receiver, the signal is given by

$$x_k = s_k + n_k. \tag{9}$$

where $\{n_k\}$ is a white noise process with power P_n. Using $\mathbf{\Phi}_k^s$ from above, the input autocovariance matrix can be written as

$$\mathbf{\Phi}_k^x = P_n \mathbf{V}^k \mathcal{D} \mathbf{V}^{*k} \tag{10}$$

where

$$\mathcal{D} = [\mathbf{I} + \rho \mathbf{R} \otimes (\bar{\mathrm{D}} \bar{\mathrm{D}}^H)], \tag{11}$$

and $\rho = \frac{P_s}{P_n}$ is the input signal to noise ratio (SNR). For the deterministic chirp result, the stationary signal being chirped is a constant DC signal. Thus setting the elements of the normalized correlation matrix $(\mathbf{R})_{i,j} = 1$ gives the chirped result in [4].

Similarly, the cross correlation vector ($\bar{\theta}_k^f$) for the one-step forward predictor is given by

$$\bar{\theta}_k^f = E[x_k \bar{\mathrm{x}}_k^*] = P_s \mathbf{V}^k (\bar{\mathrm{r}} \otimes \bar{\mathrm{D}}), \tag{12}$$

where $\bar{\mathrm{r}} = [r_1, r_2, \ldots, r_{M+1}]^T$ (the second column of $\mathbf{R}$) is the normalized one-step cross correlation vector of the stationary process. Similarly the deterministic chirp result is obtained when $\bar{\mathrm{r}} = [1, \ldots, 1]^T$.

3 Wiener Filter

The optimum Wiener weights are found by solving the Wiener-Hopf equations using the definitions of $\mathbf{\Phi}_k^x$ and $\bar{\theta}_k^f$ defined in Section 2, to give

$$\bar{\mathrm{W}}_k^0 = (\mathbf{\Phi}_k^x)^{-1} \bar{\theta}_k^f. \tag{13}$$

Fortunately these Wiener weights can be related to those of the stationary signal [6]

$$\bar{\mathrm{W}}_k^0 = \mathbf{V}^k \left[\bar{\mathrm{W}}^0 \otimes \bar{\mathrm{D}}\right], \tag{14}$$

where $\bar{\mathrm{W}}^0$ is the Wiener weight vector when the signal is stationary.

4 RLS Filter

The RLS algorithm solves for the optimum filter weights using an exponentially weighted estimate of the input auto- and cross-correlation. The algorithm estimates the autocorrelation using

$$\mathbf{R}_k = \sum_{i=1}^{k} \lambda^{k-i} \bar{\mathrm{x}}_i^* \bar{\mathrm{x}}_i^T, \tag{15}$$

where $\bar{\mathrm{x}}_k = [x_{k-1}, \ldots, x_{k-M}]^T$ and the cross correlation using

$$\bar{P}_k = \sum_{i=1}^{k} \lambda^{k-i} \bar{\mathrm{x}}_i^* x_k, \tag{16}$$

although in more computationally efficient forms. Finally, the Wiener-Hopf equation is solved to find the optimum weights

$$\bar{\mathrm{W}}_k = \mathbf{R}_k^{-1} \bar{P}_k, \tag{17}$$

where the filter is recursively updated using

$$\bar{\mathbf{W}}_k = \bar{\mathbf{W}}_{k-1} + e(k)\mathbf{R}_k^{-1}\bar{\mathbf{x}}_k^* \tag{18}$$

and $e(k)$ is the output error, given by

$$e(k) = x_k - \bar{\mathbf{x}}_k^T \bar{\mathbf{W}}_{k-1}. \tag{19}$$

4.1 Filter Misadjustment

It is shown in [6] that under the "slow-adaptation" ($\beta M \ll 2$) and "slow-variation" ($M\psi \ll \beta$) assumptions, $\mathbf{R}_k$ is quasi-deterministic. This greatly simplifies the analysis, allowing $\mathbf{R}_k$ to be moved outside of the expectations.

Using the approximations on $\mathbf{R}_k$ and λ, the noise misadjustment can be shown to be

$$\mathcal{M}_{k+1}^n = \frac{\beta}{2} M \xi_0, \tag{20}$$

where $\beta = 1 - \lambda$. This is the same form as for stationary signals.

The mean lag filter is shown to be

$$\Delta_k = -\frac{1}{\beta}\mathbf{V}^{k+1}\mathbf{\Lambda}(\bar{\mathbf{W}}^0 \otimes \bar{\mathbf{D}}). \tag{21}$$

where $\mathbf{\Lambda} = (\mathbf{I} - \mathbf{V}^*)$. The mean lag misadjustment can be written in terms of the stationary process components $(\bar{\mathbf{W}}^0, \mathbf{\Phi}^x)$ to give

$$\mathcal{M}_{k+1}^{\Delta} = \frac{\kappa}{\beta^2}\psi^2 \tag{22}$$

where

$$\kappa = (\mathbf{\Lambda}\bar{\mathbf{W}}^0)^H \mathbf{\Phi}^x (\mathbf{\Lambda}\bar{\mathbf{W}}^0)/\psi^2, \qquad M\psi \ll \beta \tag{23}$$

is the "*normalized lag misadjustment*"[1] for a chirped process. Figure 1 plots the filter transfer function at two different times for an AR1 process. It can be seen that as β decreases the mean lag component of the filter increases. Figure 3 shows the normalized lag misadjustment for an AR1 process. It can be seen that as the bandwidth increases the lag misadjustment decreases.

4.2 Optimal Adaptation Constant β_{opt}

The adaptation parameter β can now be optimized to reduce the filter misadjustment. The total misadjustment is given by

$$\mathcal{M} = \frac{\beta M}{2}\xi_0 + \frac{\psi^2}{\beta^2}\kappa \tag{24}$$

[1]The term ψ^2 is isolated since, for small ψ the matrix $\mathbf{\Lambda}$ is proportional to ψ.

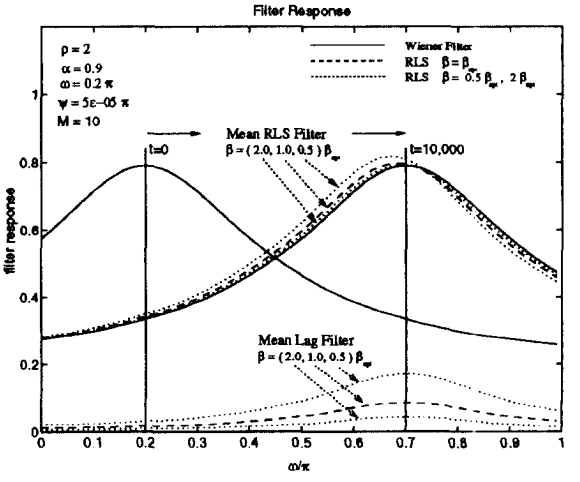

Figure 1: Filter transfer function over time for a chirped AR1 process.

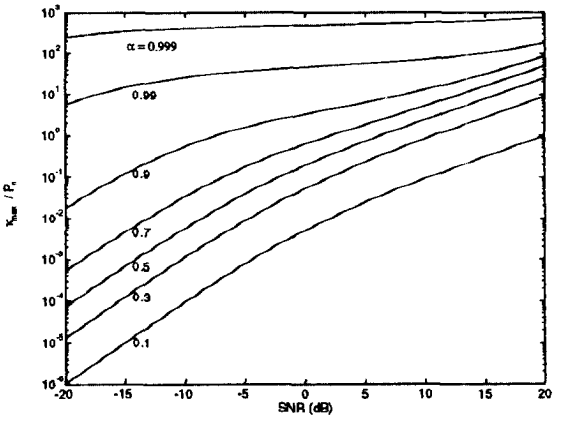

Figure 2: Normalized lag misadjustment κ_{max}/P_n vs. SNR for various AR1 correlation values (α) and $M \rightarrow \infty$.

Solving for the minimum with respect to β, the optimum adaptation constant is found to be

$$\beta_{opt} = \left(\frac{4\psi^2}{M}\right)^{1/3}\left(\frac{\kappa}{\xi_0}\right)^{1/3}. \tag{25}$$

The parameters of the *stationary* process are contained in the ratio $(\kappa/\xi_0)^{1/3}$, and this ratio is the only quantity which needs to be recalculated when a different signal is chirped. Note that β_{opt} increases with the chirp rate ψ, in order to put more emphasis on the current data. For an AR1 process, it is seen in Figure 3 that the signal dependent parameter reaches a maximum when the filter length M is increased. Note that for a deterministic chirp $\alpha = 1$, β_{opt} increases without bound as the filter length M increases, while for

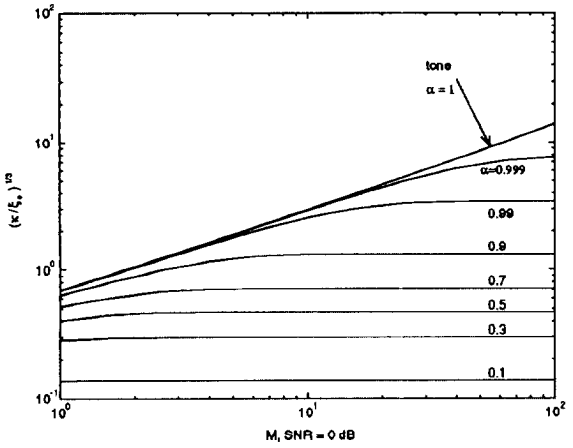

Figure 3: The signal dependent parameter $(\kappa/\xi_0)^{1/3}$ of β_{opt} versus the filter length (M) at SNR = 0dB for an AR1 process.

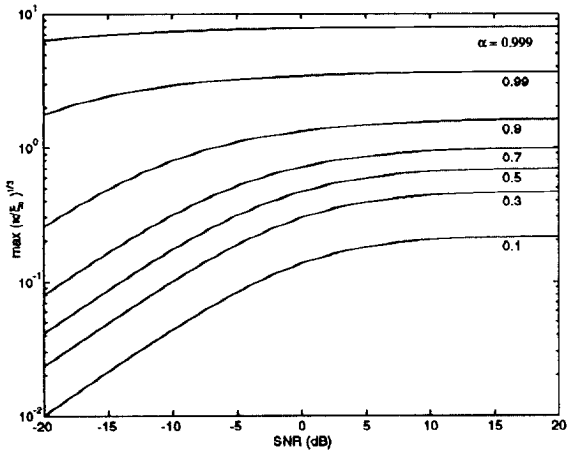

Figure 4: $\max_{M} (\kappa/\xi_0)^{1/3}$ vs. SNR for an AR1 process.

$\alpha > 0$ the parameter reaches a limit. Figure 4 plots this maximum for various input SNR.

The minimum misadjustment is

$$\mathcal{M}_{min} = \frac{3}{4} M \xi_0 \beta_{opt}. \quad (26)$$

When $\beta = \beta_{opt}$, the mean lag misadjustment is 1/2 of the noise misadjustment. Thus for a given chirp rate, if $\beta = \beta_{opt}(\psi)$ then the total misadjustment will only increase by a factor of 3/2 from the stationary cases when the signal is chirped at rate ψ.

5 Performance

Several simulations have been performed using the chirped AR1 process

$$s_k = \alpha \Omega \Psi^{-1/2} \Psi^k s_{k-1} + u_k. \quad (27)$$

β	$[\frac{1}{10}, \frac{1}{5}, \frac{1}{2}, 1, 2, 5, 10]\beta_{opt}$
ρ	2, 32
α	.5, .9 , .99, .995
ω	$.2\pi$
ψ	$[5, .5]\pi 10^{-5}$
M	3, 10

Table 1: Simulation Parameters

and BPSK signal

$$s(k) = \sqrt{2P_s} b_{k/T} \cos(\omega k + \psi k^2/2). \quad (28)$$

for both stationary ($\psi = 0$) and chirped versions ($\psi = \psi_0$). The BPSK is demodulated using an I and Q channel to give the real and imaginary parts. The AR1 process models the BPSK signal when $\alpha = 1 - 1/T$. An RLS filter was applied to both sequences and the *misadjustment ratio* was calculated using ξ/ξ_0, where[2] $\xi = E|e(k)|^2$. Simulations were performed with combinations of parameters shown in Table 1. As all results were qualitatively similar, the case ($M = 10, \rho = 2, \alpha = 0.9, \omega = 0.2\pi, \psi = 5 * 10^{-4}\pi$) is used to illustrate the results. The weights were initialized to the optimum weights and the simulation was performed for 10,000 iterations.

Figure 5 and Figure 6 plot the misadjustment of the RLS filter for the BPSK signal and its AR1 model, averaged over 10 runs.[3] For the BPSK signal the minimum recovery error, minimum estimation error and output recovery SNR are $\eta^2 = 1.3613$, $\xi_0 = 2.3613$, and $\rho_0 = 1.4619$. The AR1 model gives $\eta^2 = 1.3594$, $\xi_0 = 2.3594$, and $\rho_0 = 1.4713$. The main difference is that β_{opt} is slightly larger for the BPSK process. This is because the BPSK correlation falls off linearly, whereas the AR1 decreases exponentially. This results in an increased normalized lag (κ) for the BPSK (see Eq. 23). Thus the AR1 model generally provides a very good estimate of filter performance for the BPSK signal.

The symbols on the plots denote the simulation results, the vertical bars are the $\pm\sigma$ error bars, and the solid lines are the theoretical results. The effect of the adaptation parameter (β) on the misadjustment is seen from the two main regions on the plots:

[2]The ξ_0 used for normalization in the plots was measured using the *stationary* input sequence and the optimum Wiener filter computed from the data sequence. This is used instead of the theoretical ξ_0, to smooth the variations caused by the short runlengths used prevent the spectrum from wrapping around.

[3]The theoretical noise misadjustment used in Figure 5 and Figure 6 is taken from [3] which is more accurate for large values of β.

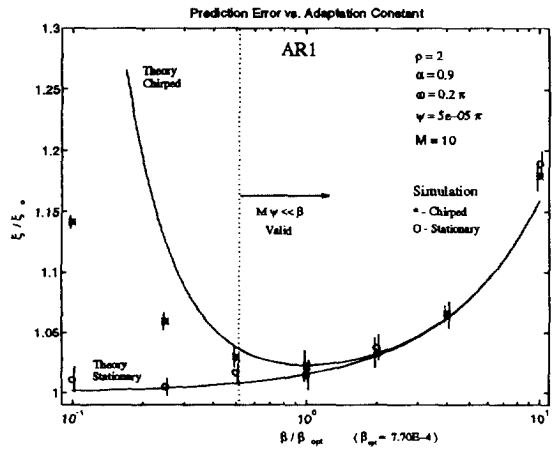

Figure 5: Misadjustment ratio (ξ/ξ_0) vs. adaptation constant (β) for a chirped AR1 process.

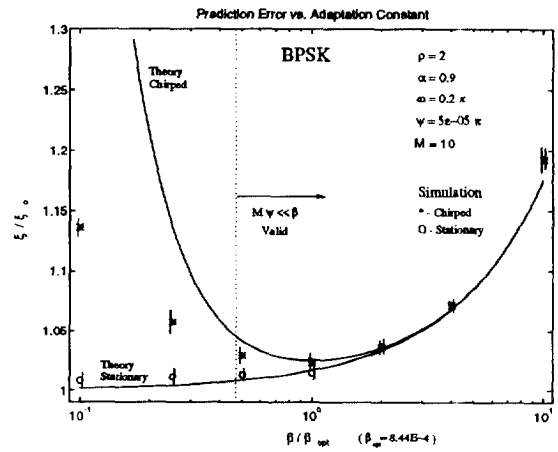

Figure 6: Misadjustment ratio (ξ/ξ_0) vs. adaptation constant β for a chirped BPSK signal.

- When $\beta \geq \beta_{opt}$, the filter tracks the chirped signal. Here the lag is negligible and the error output is *dominated* by the noise misadjustment (Figure 5,Figure 6).
- When $\beta < \beta_{opt}$, the filter is unable to track the input changes and the output error caused by the lag misadjustment is evident in Figure 5 and Figure 6.

In all cases the simulations were very close to the theoretical results near β_{opt}. Two points to note are that (1) when the adaptation parameter β becomes large, the simulation results tends to be larger than the theory for both the stationary and chirped signal, and (2) when β is too small and no longer satisfies the slow variation assumption ($M\psi \ll \beta$), the actual misadjustment is smaller than this analysis predicts.

6 Conclusion

This paper studied the performance of the RLS algorithm for a generalized chirped signal by decomposing the filter into the Wiener, lag misadjustment and noise misjustment filters. The optimum Wiener weights were derived for a *general* chirped signal, and are shown to be a chirped version of the weights for the *stationary* signal. The Wiener filter spectrum essentially shifts with the chirped signal. The lag misadjustment filter is shown to increase in magnitude as $1/\beta$, and is centered on the chirped signal. However, when added to the Wiener filter, the phases of the filter coefficients are shifted to produce a mean filter spectrum which lags the input signal.

Using the AR1 process to model a finite bandwidth signal, it is shown that the lag error *decreases* as the bandwidth increases. Simulations were performed to demonstrate the validity of the analysis for both the chirped AR1 and chirped BPSK signals. For $\beta = \beta_{opt}$, the lag misadjustment is shown to be half the noise misadjustment, hence it is possible to optimize the filter for a maximum chirp rate and have approximately the same performance when the signal is chirped at a equal or slower rate.

References

[1] S. Haykin, *Adaptive Filter Theory.* Englewood Cliffs, NJ: Prentice-Hall, 1991.

[2] B. Widrow, J. M. M. M. G. Larimore, and C. R. Johnson, "Stationary and nonstationary learning characteristics of the LMS adaptive filter," *Proceedings of IEEE*, vol. 64, pp. 1151–1162, Aug. 1976.

[3] E. Eleftheriou and D. D. Falconer, "Tracking properties and steady state performance of RLS adaptive filter algorithms," *IEEE Trans. Acoustics, Speech and Signal Processing*, vol. ASSP-34, pp. 1097–1110, Dec. 1986.

[4] O. M. Macchi and N. J. Bershad, "Adaptive recovery of a chirped sinusoid in noise,.1. performance of the RLS algorithm.," *IEEE Transactions on Acoustics, Speech, and Signal Processing*, vol. ASSP-39, pp. 583–594, Mar. 1991.

[5] O. M. Macchi and N. J. Bershad, "Adaptive recovery of a chirped sinusoid in noise,.2. performance of the LMS algorithm.," *IEEE Transactions on Acoustics, Speech, and Signal Processing*, vol. ASSP-39, pp. 595–602, Mar. 1991.

[6] P. Wei, J. Zeidler, and W. Ku, "Adaptive recovery of a chirped signal using the RLS algorithm," *Submitted to IEEE Signal Processing*, 1994.